Composites: Part B 59 (2014) 230–237

Contents lists available at ScienceDirect

Composites: Part B

journal homepage: www.elsevier.com/locate/compositesb

Analysis and design of smart mandrels using shape memory polymers

Lei Zhang [a], Haiyang Du [b], Liwu Liu [b], Yanju Liu [b,*], Jinsong Leng [a,*]

[a] *Centre for Composite Materials, Science Park of Harbin Institute of Technology (HIT), P.O. Box 3011, No. 2 YiKuang Street, Harbin 150080, People's Republic of China*

[b] *Department of Astronautical Science and Mechanics, Harbin Institute of Technology (HIT), P.O. Box 301, No. 92 West Dazhi Street, Harbin 150001, People's Republic of China*

ARTICLE INFO

Article history:
Received 27 July 2013
Accepted 29 October 2013
Available online 23 November 2013

Keywords:
A. Shape memory polymer (SMP)
C. Three-dimensional constitutive equation
C. Finite element simulation
E. Smart mandrel

ABSTRACT

Based on the thermomechanical mechanism of shape memory polymers (SMPs), the three-dimensional thermomechanical constitutive equation that can be used in the ABAQUS finite element simulation was derived. Then this paper compiled UMAT subroutine and simulated the thermomechanical behaviors of SMP smart mandrels. In addition, the properties of shape fixity and shape recovery ratio of SMP were considered in detail. Finally, filament winding experiments were proceeded on bottle-shaped and air duct-shaped mandrels and the simple and efficient demoulding of SMP mandrels were verified. The results showed the feasibility of SMP as the smart mandrels from practical application in the future.

1. Introduction

Shape memory material is one kind of smart materials, which mainly consist of shape memory alloy (SMA), shape memory polymer (SMP) and shape memory ceramics [1–3]. SMP is sensitive to some predetermined external response (such as temperature, light, electricity, magnetism and solution) and actively changes the state from a temporary shape back to the original shape [4–14]. In general, SMPs include two-phase structures: reversible phase and fixity phase, in which reversible phase can change the state between glassy and rubbery state in a particular condition to control the SMP deformation and keep a temporary shape; However, the effect of the fixity phase is to memory the original state of SMP. Compared with traditional steel materials and SMA, SMPs have the advantages of low density, low cost, good shape deformation and recoverability, ease in tailoring of transition temperature, programmability of recovery behavior. Nowadays, the application fields of SMP have covered range from aerospace to submarine, including aerospace, biomedicine, intelligent control and sensors [4–10,15–17].

With the rapid development of modern aerospace engineering, the requirement of high complexity and light weight of structures is also increasing. Traditionally, The mandrels are mostly made of multi-piece metal materials or dissolved (water-soluble or salt-soluble) materials [18–21], however, there are some disadvantages to apply these fabrication methods, such as large amount of time and energy must be invest to assemble and remove the mandrels from the fabricated composite part in multi-piece metal mandrel; the hazardous waste materials must be treated in the soluble mandrels. So some new materials and methods to improve the mandrel technology are becoming more and more importance. Researchers gradually try to apply SMP concept to the new type of mandrels development due to its good characteristics such as shape fixity and shape recovery with the change of external condition from irregular shape to be easy released. Nowadays, CRG Company has applied SMPs to develop smart mandrels with complex profiles; they completed mandrel fabrication, filament winding and demoulding process of SMPs by means of the shape memory effect [18,21]. In addition, domestic companies are starting to pay attention to the industry application of SMP materials and can be able to make simple smart mandrels [22]. Therefore, the design and manufacture of smart mandrels can be as an important direction of new technology and gradually put on the agenda.

The objective of this paper is to discuss the design method and feasibility of smart mandrels to replace the existing gypsum mandrel, multi-piece metal mandrel and dissolved mandrels. The design and fabrication technologies, the shape memory process under thermomechanical cycle, the demoulding process and reused problem of new smart mandrels are considered in detail. Moreover, the numerical simulation shows a good agreement with the experiment measurements under shape recovery process. Finally, these results can provide a detailed reference to the development of smart mandrel.

2. Theory analysis

2.1. Constitutive model

Recently, there are mainly two kinds of theories to explain the thermomechanical behaviors of SMP structures. One is based on

* Corresponding authors. Tel./fax: +86 451 86414825 (Y. Liu). Tel./fax: +86 451 86402328 (J. Leng).

E-mail addresses: yj_liu@hit.edu.cn (Y. Liu), lengjs@hit.edu.cn (J. Leng).

1359-8368/$ - see front matter © 2013 Elsevier Ltd. All rights reserved.
http://dx.doi.org/10.1016/j.compositesb.2013.10.085

the classical viscoelasticity theory, in which the structure can be seen the combination of elasticity material and viscosity materials; the other is based on phase transition theory, in which the structure include active phase and frozen phase [23–35].

Tobushi et al. [23,24] developed a constitutive model of SMP in 1997 according to the classical viscoelasticity theory, in which the standard linear viscoelastic model was modified by introduced a slip element to represent the irrecovery strain and the thermal expansion effect was considered. The curve of stress–strain–temperature relationship is expressed as follows

$$\dot{\varepsilon} = \frac{\dot{\sigma}}{E} + \frac{\sigma}{\mu} - \frac{\varepsilon - \varepsilon_s}{\lambda} + \alpha\dot{T} \tag{1}$$

where the dot denotes time derivative. The material parameters E, μ, λ, α and ε_s represent elastic modulus, viscosity, retardation time, coefficient of thermal expansion and creep irrecovery strain, respectively. σ, ε, T denote stress, strain and temperature, respectively. In addition, Yu et al. [31,32] predicted the shape recovery deformation and multi-shape thermomechanical mechanisms of SMP based on the combination of standard linear viscoelastic model and general Maxwell models.

In order to get a better characterization for SMP thermomechanical properties, Zhou et al. [33–35] rewrote Eq. (1) for three-dimensional form and the tensors were used to representation as follows

$$\varepsilon_{ij} + \lambda\dot{\varepsilon}_{ij} = \lambda(1+v)\left(\frac{\sigma_{ij}}{\mu} + \frac{\dot{\sigma}_{ij}}{E}\right) - \lambda v\left(\frac{\sigma_{kk}}{\mu} - \frac{\dot{\sigma}_{kk}}{E}\right)\delta_{ij} + (\lambda\alpha\dot{T} + \varepsilon_s)\delta_{ij} \tag{2}$$

where v and δ_{ij} represent Poisson ratio of material and Kronecker function, respectively.

The UMAT function of ABAQUS is complied in the finite simulation of SMP under complex stress conditions, the equation can be get by tensor constriction as follows

$$\sigma_{ij} + F\dot{\sigma}_{ij} = A\varepsilon_{kk}\delta_{ij} + B\varepsilon_{ij} + C\dot{\varepsilon}_{kk}\delta_{ij} + D\dot{\varepsilon}_{ij} - G \tag{3}$$

where A, B, C, D, F, G are parameters.

To convenient programming, Eq. (3) can be expressed as follows

$$\begin{cases} \sigma_{xx} + F\dot{\sigma}_{xx} = A\varepsilon_V + B\varepsilon_{xx} + C\dot{\varepsilon}_V + D\dot{\varepsilon}_{xx} - G \\ \sigma_{yy} + F\dot{\sigma}_{yy} = A\varepsilon_V + B\varepsilon_{yy} + C\dot{\varepsilon}_V + D\dot{\varepsilon}_{yy} - G \\ \sigma_{zz} + F\dot{\sigma}_{zz} = A\varepsilon_V + B\varepsilon_{zz} + C\dot{\varepsilon}_V + D\dot{\varepsilon}_{zz} - G \\ \sigma_{xy} + F\dot{\sigma}_{xy} = B\varepsilon_{xy} + D\dot{\varepsilon}_{xy} - G \\ \sigma_{yz} + F\dot{\sigma}_{yz} = B\varepsilon_{yz} + D\dot{\varepsilon}_{yz} - G \\ \sigma_{zx} + F\dot{\sigma}_{zx} = B\varepsilon_{zx} + D\dot{\varepsilon}_{zx} - G \end{cases} \tag{4}$$

At the same time, the derivative of stress and strain can be replaced by finite different method; the result can be expressed as follows

$$\begin{aligned} &\dot{f}_{t+\frac{1}{2}\Delta t} = \tfrac{\Delta f}{\Delta t} \\ &f_{t+\frac{1}{2}\Delta t} = f_t + \tfrac{\Delta f}{2} \end{aligned} \tag{5}$$

where f, Δt and Δf denote some special function, time increment step and function increment, respectively.

$$\begin{cases} (F+\frac{\Delta t}{2})\Delta\sigma_{xx} = (\frac{B}{2}\Delta t + D)\Delta\varepsilon_{xx} + (\frac{A}{2}\Delta t + C)\Delta\varepsilon_V + (A\varepsilon_V + B\varepsilon_{xx} - \sigma_{xx} - G)\Delta t \\ (F+\frac{\Delta t}{2})\Delta\sigma_{yy} = (\frac{B}{2}\Delta t + D)\Delta\varepsilon_{yy} + (\frac{A}{2}\Delta t + C)\Delta\varepsilon_V + (A\varepsilon_V + B\varepsilon_{yy} - \sigma_{yy} - G)\Delta t \\ (F+\frac{\Delta t}{2})\Delta\sigma_{zz} = (\frac{B}{2}\Delta t + D)\Delta\varepsilon_{zz} + (\frac{A}{2}\Delta t + C)\Delta\varepsilon_V + (A\varepsilon_V + B\varepsilon_{zz} - \sigma_{zz} - G)\Delta t \\ (F+\frac{\Delta t}{2})\Delta\sigma_{xy} = \frac{1}{2}(\frac{B}{2}\Delta t + D)\Delta\gamma_{xy} + \left(\frac{1}{2}B\gamma_{xy} - G - \sigma_{xy}\right)\Delta t \\ (F+\frac{\Delta t}{2})\Delta\sigma_{yz} = \frac{1}{2}(\frac{B}{2}\Delta t + D)\Delta\gamma_{yz} + \left(\frac{1}{2}B\gamma_{yz} - G - \sigma_{yz}\right)\Delta t \\ (F+\frac{\Delta t}{2})\Delta\sigma_{zx} = \frac{1}{2}(\frac{B}{2}\Delta t + D)\Delta\gamma_{zx} + (\frac{1}{2}B\gamma_{zx} - G - \sigma_{zx})\Delta t \end{cases} \tag{6}$$

Its corresponding Jacobian matrix can be expressed as follows

$$J = \begin{bmatrix} \frac{2(C+D)+(A+B)\Delta t}{2F+\Delta t} & \frac{2C+A\Delta t}{2F+\Delta t} & \frac{2C+A\Delta t}{2F+\Delta t} & 0 & 0 & 0 \\ \frac{2C+A\Delta t}{2F+\Delta t} & \frac{2(C+D)+(A+B)\Delta t}{2F+\Delta t} & \frac{2C+A\Delta t}{2F+\Delta t} & 0 & 0 & 0 \\ \frac{2C+A\Delta t}{2F+\Delta t} & \frac{2C+A\Delta t}{2F+\Delta t} & \frac{2(C+D)+(A+B)\Delta t}{2F+\Delta t} & 0 & 0 & 0 \\ 0 & 0 & 0 & \frac{2D+B\Delta t}{4F+2\Delta t} & 0 & 0 \\ 0 & 0 & 0 & 0 & \frac{2D+B\Delta t}{4F+2\Delta t} & 0 \\ 0 & 0 & 0 & 0 & 0 & \frac{2D+B\Delta t}{4F+2\Delta t} \end{bmatrix} \tag{7}$$

The classical linear viscoelastic constitutive model is carried out in the paper, the equations are extended into three-dimensional form and transformed into finite element analysis matrix with the help of finite difference method (FDM), then, the UMAT program is compiled and the thermomechanical behaviors are simulated in the paper.

2.2. Mandrels material parameters

The material of smart mandrels is styrene-based SMP. The shape memory styrene resin is assumed to be isotropic polymer material at room temperature (far less than T_g temperature) and rubber of hyperelastic material at high temperature (higher than T_g temperature above 30 °C). The typical thermomechanical cycle properties are simulated in the paper, the nonlinear properties of SMP material must be considered in finite element simulation.

The material parameters and temperature relationship developed by Tobushi in 1996 [23,24] can be expressed as follows

$$X = X_g \exp\left[k\left(\frac{T_g}{T} - 1\right)\right] \tag{8}$$

where X denotes every material parameter, X_g is the value of X at $T = T_g$, k is a constant parameter.

Zhou et al. [35] established interpolation polynomials based on experimental data points to simulate the experiment result, expressed as follows

$$X = \frac{(T-T_g)(T-T_h)}{(T_l-T_g)(T_l-T_h)}X_l + \frac{(T-T_l)(T-T_h)}{(T_g-T_l)(T_g-T_h)}X_g + \frac{(T-T_g)(T-T_l)}{(T_h-T_g)(T_h-T_l)}X_h \tag{9}$$

where T_g is glass transition temperature, T_l and T_h are the temperatures at the starting and finishing points of the glass transition from glassy to rubbery state in SMP.

The dynamic mechanicals analysis (DMA) curve of styrene-based shape memory polymer is shown in Fig. 1. It can be shown that storage modulus starts to decrease at the temperature of

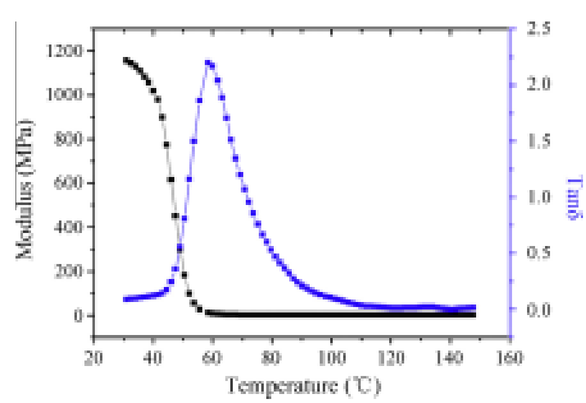

Fig. 1. DMA experiment of styrene SMP.

30 °C and end at 50 °C, the material will become rubber state after that and the modulus decrease to only a little MPa.

3. Mandrels fabrication and experimental process

In order to better understand the shape memory effect and the deformation characteristics of SMP mandrels, two kinds of additive steel molds must be fabricated in advanced. One is used to manufacture a hollow cylinder structures, which is the original state of SMP mandrel, as shown in Fig. 2, the mold is a thin-walled cylinder with outer diameter 40 mm and inner diameter 36 mm; the other kind is the pre-deformation mandrels, which include bottle-shaped steel mold and air duct-shaped steel mold. The bottle-shaped mold is an assembly structure with three components; the maximum elongation ratio is designed to 25%. The air duct-shaped mold is an assembly structure with two parts, one is circular cross section with a diameter 45 mm, another is square section with length 40 mm, the junction of the parts have an arc transition, a high precision is required in the design process of two kind of molds.

In this paper, the thermomechanical behaviors of SMP mandrels will be discussed in detailed, the structures mainly include bottle-shaped and air duct-shaped mandrels, the process of SMP “origin-deformation-recovery” is clear in Table 1.

4. Shape memory effect simulation of SMP mandrel

4.1. Bottle-shaped SMP mandrel deformation simulation

4.1.1. Design of finite element model

The subroutine UMAT is applied to simulate the SMP deformation process. The model includes two parts: the outer material is 45 steel, the inner material is styrene-based SMP, the boundary conditions is set as fixed end on the inside and outside.

Finite element unit settings, outer 45 steel is simple C3D8R unit, elastic modulus is 290 GPa, Poisson is 0.31, SMP material is C3D20H unit, the model after meshing as shown in Fig. 3. Opening the material nonlinear function database of ABAQUS, selecting various parameters and changing rule with time, running the calculation, the result of SMP displacement map is expressed as follows.

4.1.2. Radial displacement of finite element model

According to the simulation results of finite element analysis, the maximum displacement of deformed mandrel is located in the middle part, as shown in Fig. 4. The result shows that SMP has a good deformation ability, therefore the material nonlinear is considered. When the bottle-shaped is applied to fabricate structure, the middle bulging part is the most important position, which directly influence the performance of SMP mandrel.

Fig. 2. The mandrel of hollow cylinder structures.

Table 1
SMP thermomechanical behaviors analysis step setting.

Step	Loading condition	Temperature (°C)	Time (s)
1	Loading	90	1
2	Loading	90 decrease to 20	10
3	Releasing	20	1
4	Releasing	20 increase to 90	10

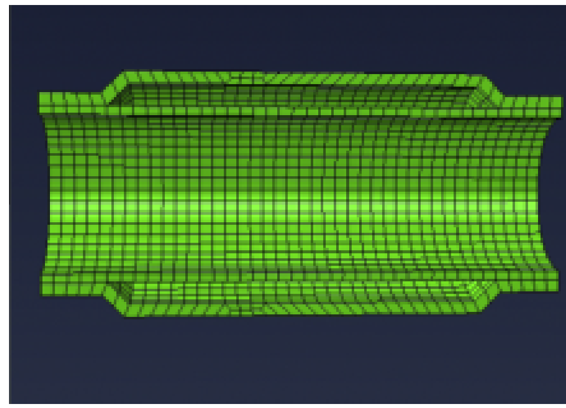

Fig. 3. The original shape of mandrel and steel model.

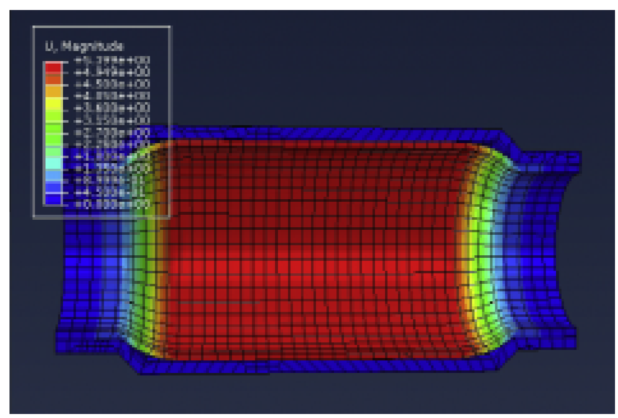

Fig. 4. The deformed shape of SMP mandrel and steel model.

To better illustrate the real working condition of the mandrel, the inner and outer surface nodes are selected to study the displacements of the SMP in deformation process.

As shown in Fig. 5(a) and (b), the maximum outer displacement of mandrel is 5 mm, located at the bulging part of the outer steel mold and the maximum inner displacement is about 5.5 mm due to the role of inner pressure. The result shows that the original resin cylindrical shape cannot be too thin, otherwise the failure ratio of mandrel will increase due to wall thickness is thinning during the deformation process.

4.1.3. Energy distribution of finite element model

The mandrel has also existed bending and tensile effect in the process of deformation, the energy for deforming is saved as strain energy at the deformed part. When deformation happens, the releasing of strain energy makes mandrel to return to the original shape, the strain energy of SMP mandrel in deformation can be expressed in Fig. 6.

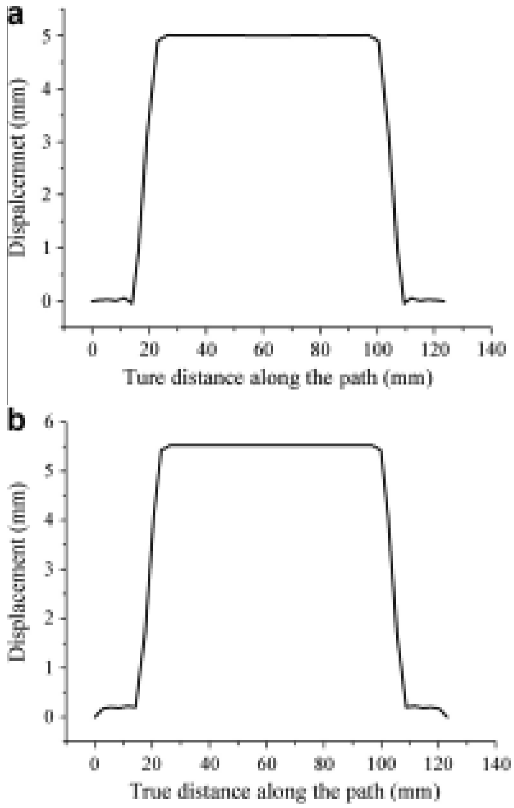

Fig. 5. (a) The outer node radical displacement curve of the mandrel. (b) The inner node radical displacement curve of the mandrel.

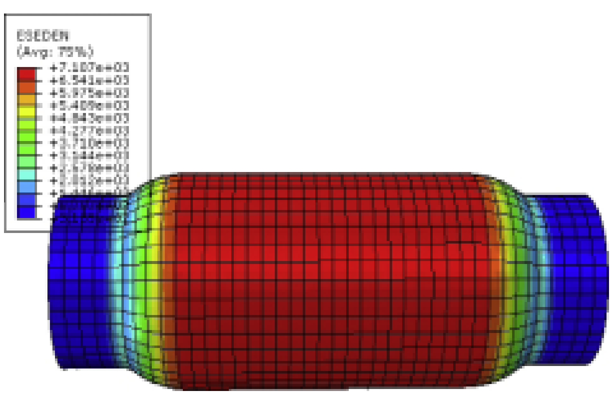

Fig. 6. The strain energy density of mandrel.

[Fig. 7](#) shows the process of energy releasing, the maximum strain energy density is located at the middle part of the mandrel. Strain energy release is an important condition for the mandrel; the total energy release relies on the central part of the mandrel recovery from the working state to the original state.

4.1.4. Shape recovery simulation of finite element model

The outer surface center node of the mandrel displacement versus time curve is shown in Fig. 8. Time 0–1, loading stage, the temperature is 90 °C, the center node displacement increases linearly with the increasing time under constant increment load until the displacement is 5 mm, Time 1–11, cooling stage, the mandrel temperature decreases slowly from above T_g to room temperature, the temperature is decreased from 90 °C to 20 °C, Time 11–12, unloading stage, the mandrel inner diameter have a small recovery during

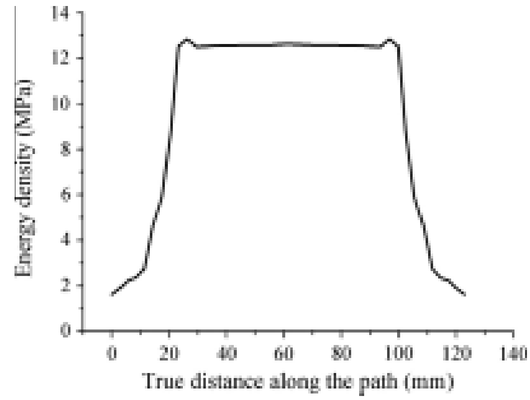

Fig. 7. The outer node strain energy density curve of mandrel.

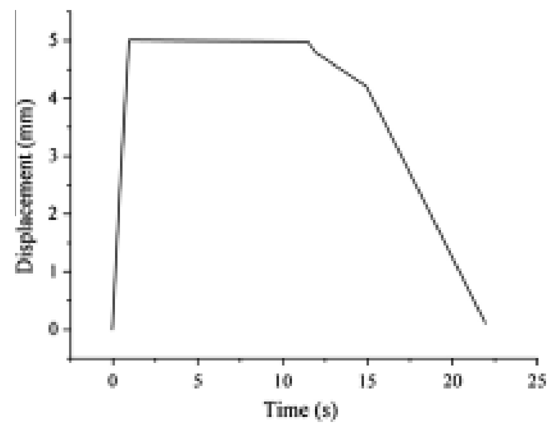

Fig. 8. The node displacement and time curve of SMP mandrel.

the stage, Time 12–22, recovery stage, the mandrel temperature is from 20 °C to 90 °C rapidly, the mandrel will recover from working state return to original state, the recovery rate is low at first, when the temperature is near to T_g, the mandrel quickly return and eventually reach the original shape.

It is well noted that the viscoelastic material has certain material damping, so a small part of strain energy will dissipate during the deformation process and the mandrel will have a certain residual strain after ultimate recovery, the residual deformation is 0.02 mm in the paper. The curve of displacement and temperature relationship is shown in Fig. 9 clearly, the original loading stage,

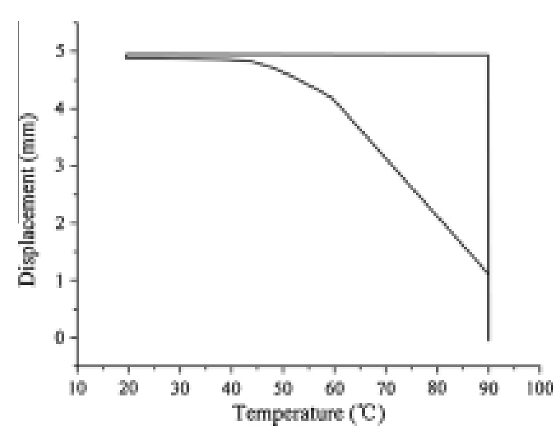

Fig. 9. The node displacement and temperature curve of SMP mandrel.

the mandrel deform to certain shape at the temperature of 90 °C, then unloading stage, the external diameter decreases 0.1 mm, the fixity ratio of the mandrel is higher than 90%, finally recovery stage, the mandrel deformation return to initial shape.

4.2. Air duct-shaped SMP mandrel shape recovery simulation

Air duct-shaped model geometric design is that square section length is 40 mm, circular section diameter is 45 mm, the rigid mandrel is applied to the initial cylinder and the pressure is 1.5 MPa, the model deformation result can be expressed in Fig. 10.

The circular cross section outer node of Air duct-shaped mandrel loading-recovery curve is shown in Fig. 11, the process is like bottle-shaped mandrel node shape recovery curve, the diameter almost keeps the maximum value and the fixity rate is higher than 90%.

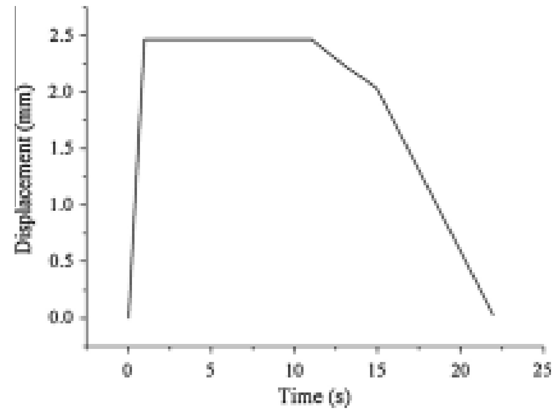

Fig. 11. The diameter recovery process of air dust-shaped mandrel.

5. Experimental analysis of SMP mandrels

5.1. Pre-deformation shapes of SMP mandrel

The bottle shaped SMP mandrel and air duct SMP mandrel experiment result as shown in Fig. 12(a) and (b). The experiment shows that the length of SMP smart mandrel is 110 mm. For bottle-shaped mandrel, the middle part is extended into circle with an outer diameter 49.80 mm, the end parts are the original shape with outer diameter 40.00 mm; For air duct-shaped mandrel, one end shape is extended into circle with an outer diameter 44.84 mm, wall thickness 1.82 mm and elongation ratio 12.5%, another end shape is square with an inner length about 39.76 mm, outer length 43.96 mm and wall thickness about 2 mm, the length ratio of the circular section and square section is 1:1.

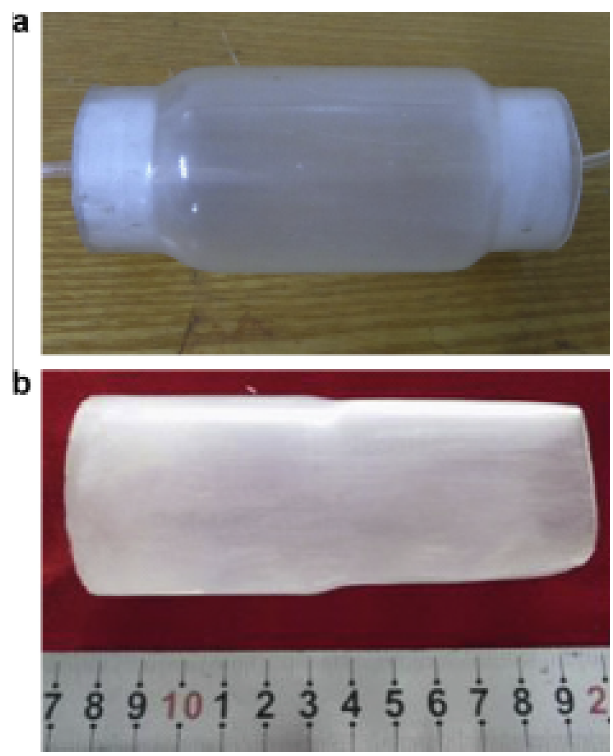

Fig. 12. (a) Pre-deformation shape of bottle-shaped SMP mandrel. (b) Pre-deformation shape of air duct-shaped SMP mandrel.

5.2. Recovery temperature and time analysis of SMP mandrel

To study the relationship between temperature and time, SMP cylinder is extended diameter by pneumatic bulging method, cooled to room temperature and kept in a temporary shape, then the SMP mandrel is placed into the adjustable constant temperature observation box, the heat sources are the resistance wires are wound all the round. The recovery experiment is set as seven high precision bottle-shaped SMP mandrels with different temperature, the change value is from 60 °C to 100 °C, SMP mandrel will be placed every other 5 °C or 10 °C, the recovery state can be got by comparing the diameter with original shape, the result is expressed in Fig. 13.

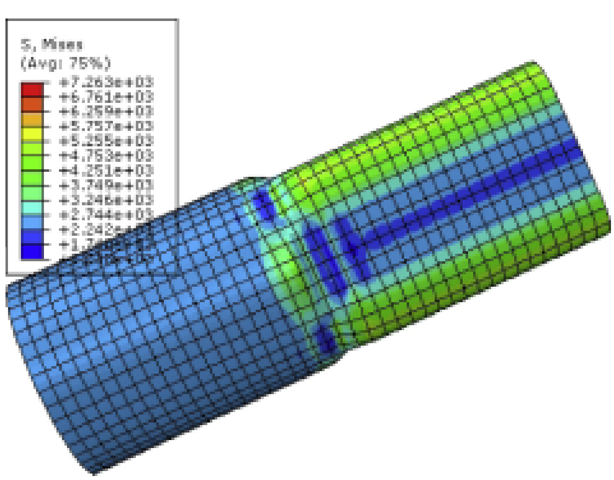

Fig. 10. The deformation of air duct-shaped mandrel.

As shown in Fig. 13, the recovery rate is high near the glass transition temperature (60 °C) of the styrene-based SMP mandrel, it will take 5 min to complete the process, the recovery rate will improve significantly with the temperature rising, when the temperature is 90 °C, the recovery time is about 70 s, however, the recovery rate has a little change when the temperature rises to 100 °C. So the ideal temperature of recovery deformation is between 90 °C and 100 °C, 90 °C is selected as a standard temperature in the experiment.

In addition, the temperature can also affect the recovery precision of the mandrel, the mandrel recovery ratio is high when the temperature is above T_g, almost achieves 100%; the recovery ratio declines when the temperature is set lower than T_g, the ratio will fall to 85% when temperature is lower 10 °C than T_g; the ratio will

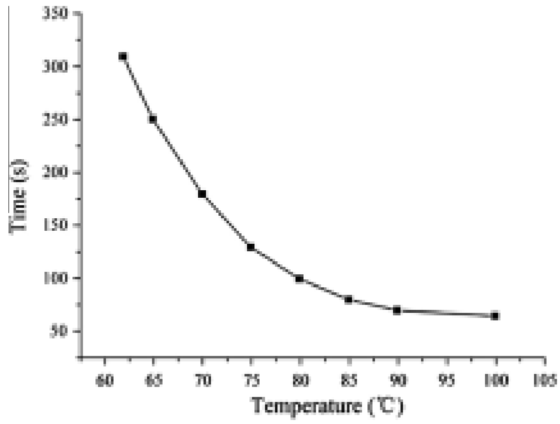

Fig. 13. Recovery time and temperature curve.

fall to 50% when temperature is lower 20 °C than T_g, moreover, there is no recovery effect when temperature is lower 30 °C than T_g.

5.3. Recovery process study of SMP mandrel

The temperature chamber is set at 90 °C to observe the recovery process of mandrel. As shown in Fig. 14, the recovery process of the mandrel can be divided into three steps. Step 1, the mandrel starts to recovery shape markedly when the temperature arrive the glass transition temperature, but the rate is slow, this is called early recovery stage; Step 2, the rate increase obviously with the temperature change when the temperature above the glass transition temperature, this is called main recovery stage; Step 3, the rate declines rapidly when the SMP mandrel shape near complete recovery. The result shows that the recovery process of the SMP mandrel is relatively smooth; there is a buffering process at the early and later stage, which reduces the risk of structure damage compared with traditional rigid mandrel, so the shape memory polymer becomes more and more application.

To better effectively understand the working mechanicals of SMP mandrel, a straight line is drawn along the axial direction on the mandrel surface and select two points are selected in the line, one point is located at the middle part, another point is located at the shoulder of the mandrel, two straight line along radial direction are drawn through the two points, they are named as The Head Line and The Middle line, the diameters change of the two lines are shown in Fig. 15.

As shown in Fig. 15, the recovery process of the SMP starts from the shoulder and then drives the middle part to recover, the recovery rate of the two parts have a little different, the reason is that the shoulder has large bend angle, belonging to the large deformation and storing large energy, when the temperature is higher than T_g, the rate of energy release is fast and recovery time is early. The decreasing diameter directly drives the middle part to recover and realize the recovery of the whole mandrel.

5.4. Recovery ratio analysis of SMP mandrel

There are creep and stress relaxation in material deformation and recovery process of SMP mandrel under high temperature environment, so the mandrel exist the dissipation of energy. The most deficiency induced by energy dissipation of SMP deformation is that the mandrel can not recover its original shape and the effect accumulates with the increasing deformation times. If the recovery accuracy cannot meet the conditions, the mandrel will affect the demoulding performance of the mandrel and cause the mandrel failure finally. To discuss the recovery mechanics of the SMP mandrel, multiple deformation and recovery experiment have be carried out under the same condition, the vernier caliper is applied to measure the diameter of the recovered mandrel, the average value of three different positions on the outer surface of mandrel is selected as the experimental result.

Recovery ratio formula has been proposed to characterize the recovery performance of the mandrel, in which the initial diameter of SMP hollow cylinder is D_0 ($D_0 = 39.76$ mm), the first time deformed maximum diameter is D_1, then the measured value after deformation recovery is D', so the recovery ratio can be expressed as follows

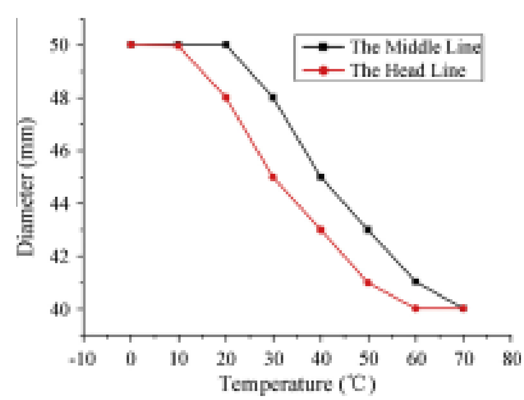

Fig. 15. The diameter change curve of SMP mandrel.

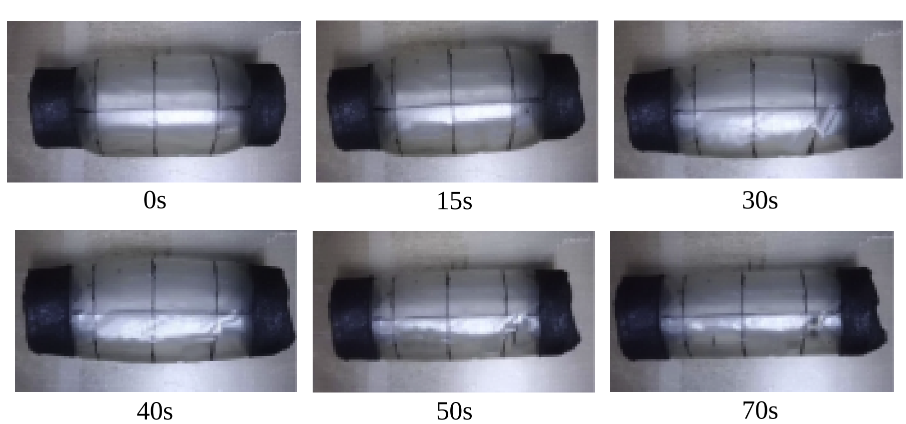

Fig. 14. The recovery process of bottle-shaped SMP mandrel.

$$R = \left(1 - \frac{D' - D_0}{D_1 - D_0}\right) \times 100\% \quad (10)$$

The relationship between diameter and recovery times can be curved in Fig. 16.

As shown in Fig. 16, the diameter of SMP mandrel after multiple deformation increase nearly linearly, the residue strain will exist after every deformation recovery and increase with the recovery time obviously. As shown in Fig. 17, the recovery ratio of the SMP mandrel achieves 98% after the first three times, but it reduces fast after that, this is consistent with the finite element analysis, the reason is that the styrene SMP mandrel appears flaw and the accumulation of creep effect between the deformation and recovery process.

It is noted that the deformation state of SMP mandrel is easy to damage due to some defects in the fabrication process. In addition, the SMP mandrel will local damage during 10–15 times working cycles in experiment. Obviously, the disadvantage of lower recovery ratio still need study and improve in the future work.

5.5. Demoulding verification of SMP mandrel

The original shape of SMP mandrel is a thin-walled hollow cylinder with outer diameter of 40 mm and inner diameter of 36 mm. After the steps of high temperature deformation and shape fixity, the SMP mandrel will keep a temporary state to satisfied filament winding. Finally, the demoulding feasibility must be considered to fabricate the production. In the paper, the bottle-shaped SMP mandrel and air duct-shape SMP mandrel have shown a good demoulding processing as shown in Fig. 18(a) and (b) [36]. The diameter change after experiments can be shown in Table 2.

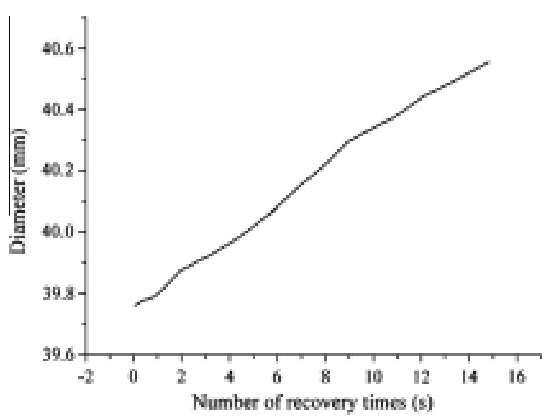

Fig. 16. Recovery times and diameter curve.

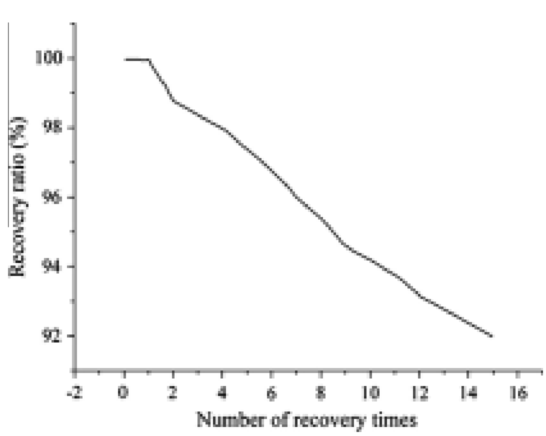

Fig. 17. Recovery time and recovery ratio curve.

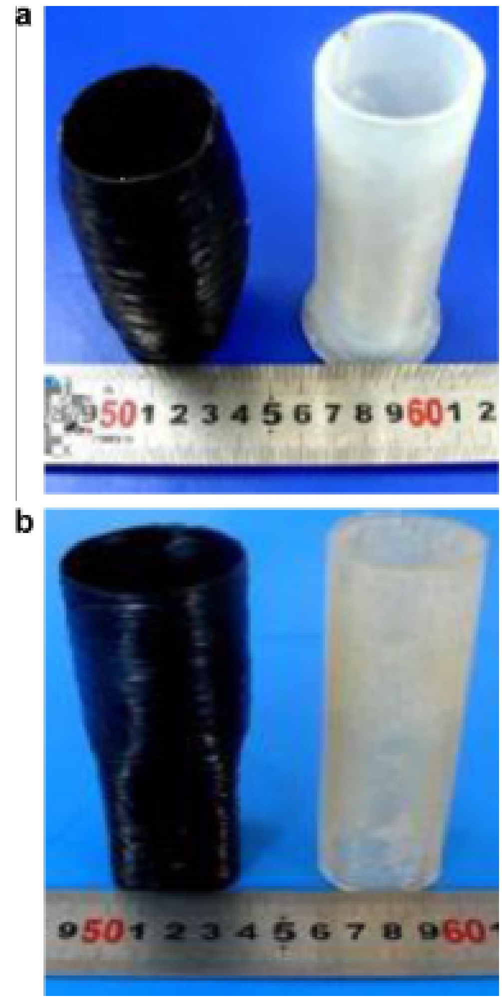

Fig. 18. (a) The demoulding result of bottle-shaped SMP mandrel [36]. (b) The demoulding result of air duct-shaped SMP mandrel [36].

Table 2
SMP diameter measurement after experiment.

Mandrel	Bottle-shaped SMP mandrel			Air duct-shaped SMP mandrel		
	1	2	3	1	2	3
D_1/mm	40.02	40.06	40.02	40.04	40.06	40.06
D_2/mm	40.04	40.02	40.04	40.08	40.10	40.10

Experiment shows that mandrels can release the winding composite part and recover the original shape after some time. The recovery ratio of bottle-shaped SMP mandrel and air duct-mandrel are higher than 90%, this fact shows that the feasibility of SMP as a smart mandrel and fully reflects the excellent demoulding performance.

6. Conclusions

This paper is mainly based on the unique advantages of SMP smart materials, such as large deformation, high shape fixity and shape recovery ratio, applies finite element simulation and experimental results to show the feasibility of SMP as a new kind of smart mandrels, In addition, demoulding experiment is used to verify the effectivity, some conclusions can be got as follows.

(1) Based on the thermomechanical behaviors of SMPs, the three-dimensional thermomechanical constitutive equation that can be used in ABAQUS was derived. The simulation results of thermomechanical cycle show that the SMP material is feasible as a smart mandrel in theory.
(2) This paper verify the feasibility of SMP as a smart mandrel from experimental application based on two kinds of special structures, bottle-shaped mandrel and air duct-shaped mandrel, some experiments are carried out to verify the recovery and deformation properties, including the best recovery temperature, recovery time, recovery ratio, and so on.
(3) The demoulding technology can be also verified in the paper. However, there are much room to improve the design of reusable SMP mandrels in the future study. So developing better excellent performance SMP mandrels and designing better precision rigid outer mold will become an important direction of future study work.

Acknowledgements

This work is supported by the National Natural Science Foundation of China (Grant Nos. 1122521, 11272106, 11102052).

References

[1] Wei ZG, Sandstrom R, Miyazaki S. Shape memory materials and hybrid composites for smart systems – part I shape memory materials. J Mater Sci 1998;33(15):3743–62.
[2] Hornbogen E. Comparison of shape memory metals and polymers. Adv Eng Mater 2006;8(1–2):101–6.
[3] Hartl DJ, Chatzigeorgiou G, Lagoudas DC. Three-dimensional modeling and numerical analysis of rate-dependent irrecoverable deformation in shape memory alloys. Int J Plast 2010;26(10):1485–507.
[4] Behl M, Lendlein A. Shape-memory polymers. Mater Today 2007;10:20–8.
[5] Xiao Y, Zhou SB, Wang L, Zheng XT, Gong T. Crosslinked poly (e-caprolactone)/poly (sebacic anhydride) composites combining biodegradation, controlled drug release and shape memory effect. Composites: Part B 2010;41(7):531–42.
[6] Liu C, Qin H, Mather PT. Review of progress in shape memory polymers. J Mater Chem 2007;17:1543–58.
[7] Huang WM, Ding Z, Wang CC, Wei J, Zhao Y, Purnawali H. Shape memory materials. Mater Today 2010;13(7–8):54–61.
[8] Xie T. Tunable polymer multi-shape memory effect. Nature 2010;464(7286):267–70.
[9] Leng JS, Lan X, Liu YJ, Du SY. Shape memory polymers and their composites: stimulus methods and applications. Progr Mater Sci 2011;56(7):1077–135.
[10] Hu JL, Zhu Y, Huang HH, Lu J. Recent advances in shape memory polymers: structures, mechanism, functionality, modeling and applications. Progr Polym Sci 2012;37(12):1720–63.
[11] Liu Y, Gall K, Dunn ML, McCluskey P. Thermomechanics of shape memory polymer nanocomposites. Mech Mater 2004;36(10):929–40.
[12] Schmidt AM. Electromagnetic activation of shape memory polymer networks containing magnetic nanoparticles. Macromol Rapid Commun 2006;27(14):1168–72.
[13] Lendlein A, Jiang HY, Junger O, Langer R. Light-induced shape-memory polymers. Nature 2005;434:879–82.
[14] Lv HB, Leng JS, Liu YJ, Du SY. Shape-memory polymer in response to solution. Adv Eng Mater 2008;10:592–5.
[15] Keusch P, Greer D, Rozembersky J. NASA contactor report 1969. [NASA CR-1384].
[16] Baghani M, Naghdabadi R, Arghavani J. A semi-analytical study on helical springs made of shape memory polymer. Smart Mater Struct 2012;21(4):045014.
[17] Zhu GM. Shape memory polymer and application. Beijing: Chemical Industry Press; 2002. p. 26–45.
[18] Everhart MC, Nickerson DM, Hreha RD. High-Temperature Reusable Shape Memory Polymer Mandrels, Smart Structures and Materials 2006: Industrial and Commercial Applications of Smart Structures Technologies. In: Proc. of SPIE; 2006, p. 6171: 61710K.
[19] Mallick K, Tupper ML, Arritt BJ, Chris L, Paul C. Thermo-micromechanics of microcracking in a cryogenic pressure vessel. In: 44th AIAA/ASME/ASCE/AHS/ASC Structures, Structural Dynamics, and Materials Conference, Norfolk, Virginia; April 7–10, 2003.
[20] Mallick K, John C, Ryan K, Steven A, Naseem M, Paul C, et al. An integrated systematic approach to linerless composite tank development. In: 46th AIAA/ASME/ASCE/AHS/ASC structures, structural dynamics, and materials conference, Austin, Texas; April 18–21, 2005.
[21] Everhart MC, Stahl J. Reusable shape memory polymer mandrels, smart structures and materials 2005: industrial and commercial applications of smart structures technologies. San Diego, vol. 5762; 2005. p. 27–34.
[22] Mo J. Chinese mold assistant identify smart mold development target and key projects. China Industry Press; 2011.
[23] Tobushi H, Hara H, Yamada E, Hayashi S. Thermomechanical properties in a thin film of shape memory polymer of polyurethane series. Smart Mater Struct 1996;5:483–91.
[24] Tobushi H, Hashimoto T, Hayashi S, Yamada E. Thermomechanical constitutive modeling in shape memory polymer of polyurethane series. J Intell Mater Syst Struct 1997;8:711–8.
[25] Tobushi H, Okumura K, Hayashi S, Norimitsu I. Thermomechanical constitutive model of shape memory polymer. Mech Mater 2001;33:545–54.
[26] Lin JR, Chen LW. The mechanical-viscoelastic model and WLF relationship in shape memorized linear ether-type polyurethanes. J Polym Res 1999;6(1):35–40.
[27] Lin JR, Chen LW. Shape-memorized crosslinked ester-type polyurethanes and its mechanical viscoelastic model. J Appl Polym Sci 1999;73:1305–19.
[28] Li FK, Larock RC. New soybean oil-styrene-divinylbenzene thermosetting copolymers. v. shape memory effect. J Appl Polym Sci 2000;84(8):1533–43.
[29] Abranhamson ER, Lake MS, Munshi NA, Gall K. Shape memory mechanics of an elastic memory composite resin. J Intell Mater Syst Struct 2003;14(10):623–32.
[30] Nguyen TD, Qi HJ, Castro F, Long KN. A thermoviscoelastic model for amorphous shape memory polymers: incorporating structural and stress relaxation. J Mech Phys Solids 2008;56(9):2792–814.
[31] Ge Q, Yu K, Ding YF, Qi HJ. Prediction of temperature-dependent free recovery behaviors of amorphous shape memory polymers. Soft Matter 2012;8(43):11098–105.
[32] Yu K, Xie T, Leng JS, Ding YF, Qi HJ. Mechanisms of multi-shape memory polymer and associated energy release in shape memory polymers. Soft Matter 2012;8(20):5687–95.
[33] Zhou B, Liu YJ, Leng JS, Li T. Study on thermo-mechanicals behaviors of shape memory polymer. Key Eng Mater 2010;419–420:497–500.
[34] Zhou B, Liu YJ, Leng JS. A macro-mechanical constitutive model of shape memory polymer. Sci China Phys Mech Astronom 2010;40(7):896–903.
[35] Zhou B, Liu YJ, Leng JS. Finite element analysis on thermomechanical behavior of styrene based shape memory polymers. Acta Polymer Sinica 2009;9(6):525–9.
[36] Leng JS, Liu LW, Lv HB, Liu YJ. Applications for shape memory polymer composite in aerospace. JEC Compos 2012;72:56–8.